Science of the Total Environment 744 (2020) 140809

Contents lists available at ScienceDirect

Science of the Total Environment

journal homepage: www.elsevier.com/locate/scitotenv

Mitigating rural WWTP impacts: System dynamics modeling of downstream nutrient outputs

John F. Hallas [a], Cheryl L. Mackowiak [b], Ann C. Wilkie [a,*]

[a] Soil and Water Sciences Department, University of Florida-IFAS, Gainesville, FL 32611, USA
[b] North Florida Research and Education Center, University of Florida-IFAS, Quincy, FL 32351, USA

HIGHLIGHTS

- System dynamics modeling provides a tool for downstream nutrient load management.
- A system dynamics model was used to assess output nutrient loads at rural WWTPs.
- Intentional struvite recovery reduced effluent P discharge almost completely.
- Incorporating struvite recovery increased biosolids N:P by reducing P content.
- Effluent P and biosolids N:P reductions can mitigate the impact of WWTP discharges.

GRAPHICAL ABSTRACT

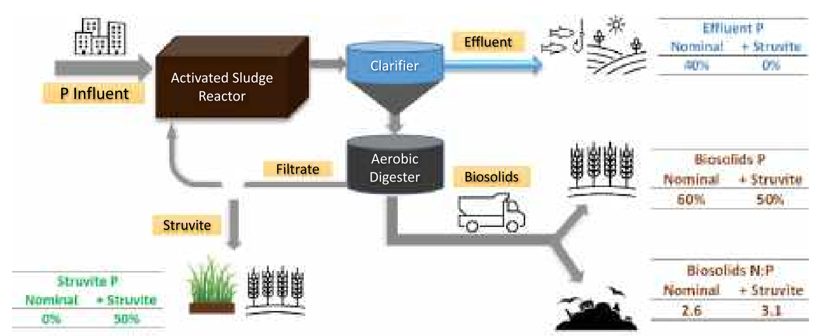

Struvite fertilizer for urban and rural use

Greater biosolids N:P reduces plant nutrients lost to landfills

ARTICLE INFO

Article history:
Received 17 May 2020
Received in revised form 4 July 2020
Accepted 6 July 2020
Available online 11 July 2020

Editor: Huu Hao Ngo

Keywords:
Biosolids
Effluent
Phosphorus
Struvite
System dynamics model
Wastewater treatment

ABSTRACT

A system dynamics modeling approach was used to assess the potential impact of intentional struvite crystallization recovery on wastewater treatment plant (WWTP) allocation of N and P in effluent and biosolids outputs. Struvite crystallization has been used to recover wastewater N and P and produce valuable fertilizer. However, it is often overlooked whether additional benefits may be realized by diverting N and P from other fates. A system dynamics model was used with operational data from three activated-sludge WWTPs in North Florida. Incorporating struvite crystallization reduced the effluent P load by 37 to 100%, dependent upon the WWTP. This may translate into substantial savings for systems facing severe restrictions in effluent P release outside the plant. Additionally, biosolids P load reductions ranged from 17 to 46%. The model also predicted a 37% average increase in the biosolids N:P ratio. Increasing the N:P ratio may allow for greater biosolids land-application rates where P fertilizer restrictions exist. In comparison, the N load reductions were much less dramatic, i.e. below 10% reduction from the effluent and 14% from the biosolids. Most N inputs into an activated-sludge type WWTP are likely lost through denitrification during wastewater processing and struvite does not appear to be a significant means of recovering N from small WWTPs. However, incorporating struvite recovery into even the simplest WWTPs reduces effluent post-treatment needs and results in a more useful biosolids product.

1. Introduction

In recent years, phosphorus (P) loads to the world's rivers have doubled because of deforestation and soil erosion, fertilizer runoff, and sewage discharge (Filippelli, 2008). Land-applied P from soluble mineral or

* Corresponding author.
E-mail address: acwilkie@ufl.edu (A.C. Wilkie).

https://doi.org/10.1016/j.scitotenv.2020.140809
0048-9697/

organic fertilizers (e.g., manures, litter, biosolids) can often move P off-site via runoff and leaching, leading to eutrophication and subsequent degradation of water bodies (Elser and Bennett, 2011; Hendriks and Langeveld, 2017).

Capturing excess municipal wastewater P through struvite ($MgNH_4PO_4 \cdot 6H_2O$) precipitation is an attractive option for P recovery and its re-use as fertilizer, but the technology has been largely limited to anaerobic wastewater treatment systems. However, Hallas et al. (2019) demonstrated that small rural wastewater treatment plants (WWTPs) with activated-sludge systems can also benefit from struvite precipitation and recovery methods, with little to no co-precipitates, if pH control and reaction chemistry (typically magnesium (Mg) augmentation) are addressed. They maintained digester pH through degassing, while Mg augmentation was supplied by adding a soluble Mg salt. Magnesium is often supplied as $MgSO_4$ or $MgCl_2$ salts (Lahav et al., 2013; Romero-Güiza et al., 2015; Zhao et al., 2019). However, the unconsumed SO_4^{2-} can increase wastewater corrosivity, as well as emit odor (Wiener et al., 2006). When wastewater effluent is used for crop irrigation, the additional SO_4^{2-} and Cl^- may also negatively impact soil solid and aqueous phase nutrient/metal balances (de Sousa et al., 2014; Khalid et al., 2018).

Without struvite crystallization, the WWTP influent P (~70%) is primarily incorporated into the sludge, which is separated from the activated-sludge process for further treatment to reduce volatile suspended solids and thereby decrease the sludge volume, reduce pathogens, and achieve vector attraction reduction (Wang et al., 2007; Hallas et al., 2015a, 2015b). Once treated, this material is designated as biosolids. Small WWTPs most often stabilize biosolids through aerobic processes that rely upon biochemical oxidation (Nowak, 2006). As a result, the aerobic digester is the major sink for P until its removal as biosolids. A relatively smaller proportion of P, approximately 30% or less, leaves the WWTP as effluent. It is unclear how intentional struvite precipitation affects the conventional P output streams, which is important from the standpoint of excessive P in one or more alternative output streams (effluent and biosolids).

For example, P reductions in effluent output are typically achieved through chemical precipitation with materials such as aluminum sulfate and treatment costs average \$309 per m^3 of wastewater (U.S. EPA, 2015). Although biosolids are a viable source of nitrogen (N) and P fertilizer (Elliott et al., 2005; Barbarick et al., 2017; Silveira et al., 2019), the N:P ratio is lower than plant demand. Over time, if biosolids applications are based on N requirements (which is the convention for many places), soil P accumulates and outpaces crop needs (O'Connor et al., 2004). Reducing biosolids P content therefore has the potential to improve biosolids marketability.

There is a long history of using struvite formation models to enhance controlled struvite precipitation and recovery, or to mitigate nuisance struvite formation in WWTP wastewater streams (Snoeyink and Jenkins, 1980; Loewenthal et al., 1994; Ohlinger et al., 1998). However, to date, there have not been reports of mass balance models that demonstrate how struvite precipitation impacts N and P in the other WWTP downstream outputs, in particular, N and P loads destined for discharge to the environment through treated wastewater effluent and biosolids. Although Venkatesan et al. (2016) developed a P mass balance model, it was limited to a single WWTP design with enhanced biological P removal and anaerobic biosolids digestion.

In this study, we used a system dynamics modeling approach to assess the impact of intentional struvite recovery on the proportioning of N and P to wastewater effluent and biosolids, using wastewater loading data from three activated-sludge WWTPs. Chloride and sulfate from magnesium augmentation (used to increase struvite yield) were also modeled, since these anions at high concentrations may pose operational or environmental risks. The system dynamics approach provides solutions to real-world systems having complex interactions, where linear and other traditional analytic approaches often prove inadequate (Martinez-Moyano, 2018).

Table 1
WWTP location operational data from 2013 to 2018.

Parameters	Location 1	Location 2	Location 3
Design type	Complete mix	SBR	SBR
Treatment capacity (m^3 d^{-1})	2650	1893	946
Average treatment rate (m^3 d^{-1})	2445	976	518
Filtrate flow rate (m^3 d^{-1})	53	37.9	18.9
Influent P (kg d^{-1})[a]	17.6 ± 4.1	7.0 ± 1.3	3.7 ± 0.7
Influent N (kg d^{-1})[a]	117.8 ± 27.7	47.0 ± 5.6	25.0 ± 4.8
Effluent P (kg d^{-1})[a]	7.0 ± 1.3	2.3 ± 0.4	2.7 ± 0.5
Effluent N (kg d^{-1})[a]	24.5 ± 5.8	9.8 ± 1.5	5.2 ± 1.0
Biosolids P (kg d^{-1})[a]	10.6 ± 0.8	4.7 ± 0.5	1.1 ± 0.1
Biosolids N (kg d^{-1})[a]	27.5 ± 1.3	9.0 ± 1.5	0.7 ± 0.1
P to biosolids conversion ratio	0.60 ± 0.09	0.67 ± 0.08	0.28 ± 0.06
Struvite (g m^{-3} d^{-1})[b]	353.1	74.4	93.8

[a] Data represent means ± standard deviation (n = 256).
[b] Adapted from Hallas et al. (2019).

2. Materials and methods

The software package Structural Thinking Experimental Learning Laboratory with Animation (STELLA) V9.0 (isee systems Inc., Lebanon, NH, USA) was used for this study. STELLA offers a means for addressing changes in P and N outputs at WWTPs using four basic building blocks. These are comprised of stocks, flows, converters and connectors: 1) stocks represent material accumulations, 2) flows are the rates that represent inputs and outputs to stocks, 3) converters are equations used to generate output values over each time interval and are used by other variables, such as flows, and 4) connectors represent dependencies between converters and flows, thereby regulating flows.

Wastewater treatment plant N, P, SO_4^{2-}, and Cl^- concentrations and their respective allocations to struvite, effluent, and biosolids were simulated as a function of wastewater input and struvite precipitation. Struvite formation rate data originated from three North Florida WWTPs, as reported by Hallas et al. (2019). These and other relevant operational data (Table 1) were input to STELLA system dynamics models.

The WWTPs represented two commonly used variations of activated-sludge wastewater treatment processing (Grady et al., 1999). Location 1 WWTP was a complete-mix reactor, with the activated sludge returned throughout the entire active sludge processing (Tchobanoglous et al., 2014), while the other two WWTPs (Locations 2 and 3) were sequencing batch reactors (SBR), with the activated-sludge process carried out in a single tank (Hallas et al., 2019). Among the three WWTPs, processing capacities ranged from 946 to 2650 m^3 wastewater d^{-1}. The influent, effluent, and biosolids data used to populate the models were compiled from operational data collected weekly from 2013 through 2018 (n = 256).

2.1. Sample analyses

Total N was calculated using standard methods SM-4500-NH_3, SM-4500-NO_3 E, SM-4500-N_{org} E (AWWA et al., 2012). Filtrate NH_4-N was measured using standard method SM-4500-NH_3 (AWWA et al., 2012); PO_4-P was measured using standard method SM-4500-P E (AWWA et al., 2012). Additionally, Cl^- and SO_4^{2-} sampling were not part of the

Table 2
Measured Cl^- and SO_4^{2-} loads.

Parameters (kg d^{-1})	Location 1	Location 2	Location 3
Influent Cl^-	116 ± 13.3[a]	30.6 ± 5.2	27.6 ± 2.0
Effluent Cl^-	112.7 ± 36.4	29.7 ± 15.8	26.7 ± 3.3
Biosolids Cl^-	3.5 ± 0.6	0.9 ± 0.3	0.8 ± 0.2
Influent SO_4^{2-}	16.7 ± 9.2	13.8 ± 6.5	1.1 ± 0.3
Effluent SO_4^{2-}	6.7 ± 2.5	5.5 ± 1.5	0.45 ± 0.1
Biosolids SO_4^{2-}	10 ± 0.8	8.3 ± 1.3	0.7 ± 0.1

[a] Data represent means ± standard deviation (n = 10).

original operational data set but were measured as composite samples collected biweekly (April to June 2019) at the three locations, using SM 4500 Cl^- C (AWWA et al., 2012) and ASTM D516-90 (ASTM International, 1995) respectively. The Cl^- and SO_4^{2-} data are given in Table 2.

2.2. Phosphorus model

Eq. (1) represents the P loading at the three WWTPs.

$$\text{Influent P load} = \text{Effluent P load} + \text{Biosolids P load} \tag{1}$$

To account for P following the separation of effluent from suspended solids, a biosolids P conversion ratio was calculated, based on the quotient of biosolids P load and influent P load (Eq. (2)). Eqs. (1) and (2) were used to populate STELLA model stocks, flows, and rates (Fig. 1).

$$\text{Biosolids P conversion ratio} = \frac{\text{Biosolids P load}}{\text{Influent P load}} \tag{2}$$

The location operational data (Table 1) were used to validate the P model. Subsequently, the struvite P load (output) was then added to the model, using rate data from Table 1. The experimentally determined rates were measured from a separate series of laboratory experiments where wastewater filtrates from each of the three WWTP locations were used to determine P removal rates due to struvite formation (Hallas et al., 2019).

2.3. Nitrogen model

A second model was used to determine the effect struvite production has on biosolids N loading and N:P ratios. Since activated-sludge WWTPs were designed for biological N removal, there is a large proportion of N input targeted for denitrification. To account for this potential loss, a total nitrogen (TN) balance was calculated, using the Activated Sludge Model 3 (ASM3) (Henze et al., 2002) (Eq. (3)). The original P model (Fig. 1) was modified for N (Fig. 2). Nitrogen data from Table 1 were used to validate the N model.

$$N_{TOT} = S_{NH_4} + S_{NO_x} + S_{N_2} + i_{NSI}S_I + i_{NSS}S_s + i_{NXS}X_s + i_{NBM}(X_H + X_A) + i_{NXI}X_I \tag{3}$$

where,

S_{NH4} = ammonium plus ammonia nitrogen (g N m^{-3})
S_{NOX} = nitrate plus nitrite nitrogen (g N m^{-3})
S_{N2} = nitrogen (g N m^{-3})
i_{NX} = fraction of nitrogen incorporated in substrate X
S_I = inert soluble organic material (g chemical oxygen demand (COD) m^{-3})
S_S = readily biodegradable organic substrates (g COD m^{-3})
X_S = slowly biodegradable organic substrates (g COD m^{-3})
X_H = heterotrophic organisms (g COD m^{-3})
X_A = nitrifying organisms (g COD m^{-3})
X_I = inert particulate organic material (g COD m^{-3}).

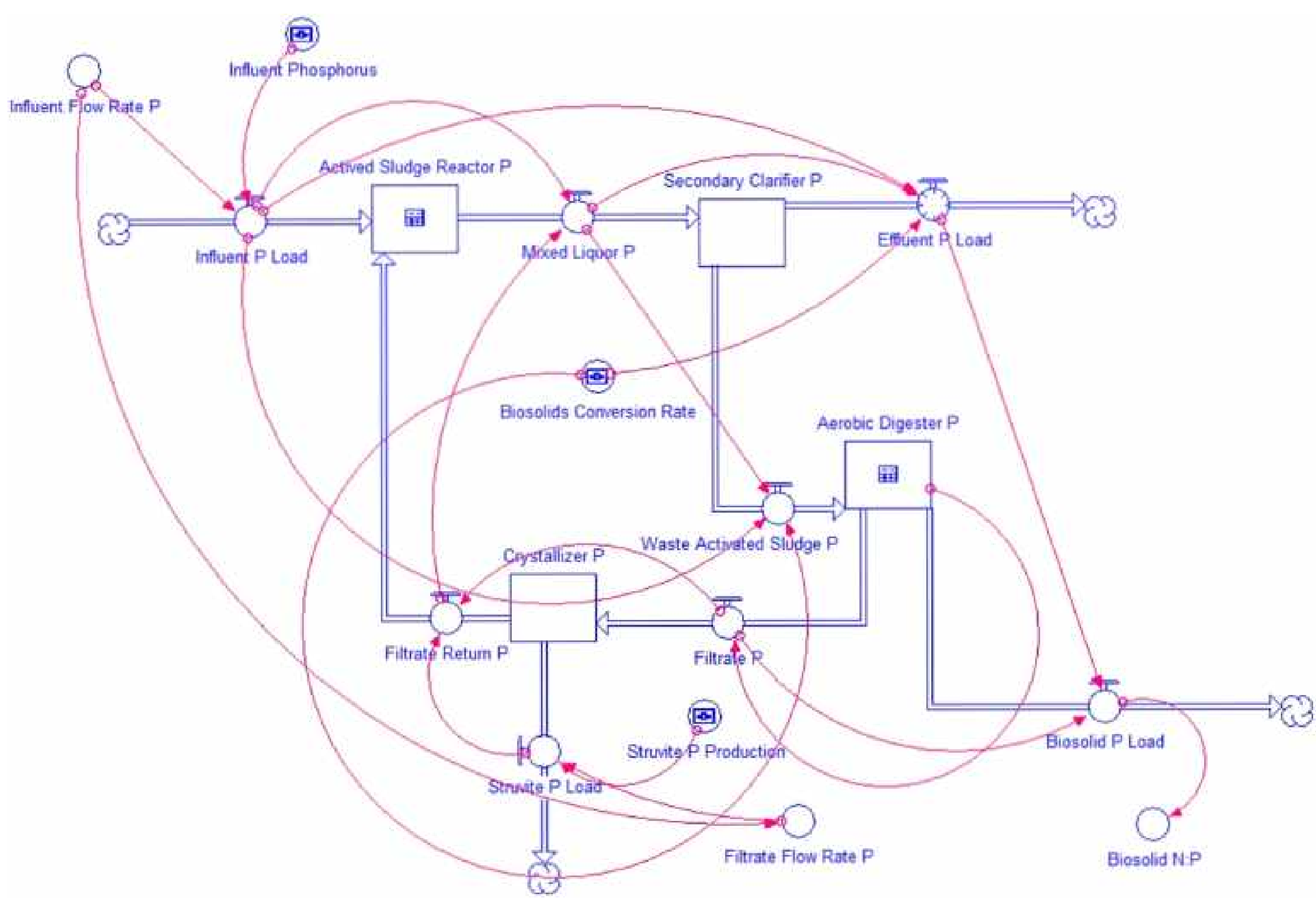

Fig. 1. Phosphorus mass balance model. Stocks (rectangle) and flows (pipe with tap) are the model's basic building blocks. Converters (small circles) represent calculations that link the flows and stock values.

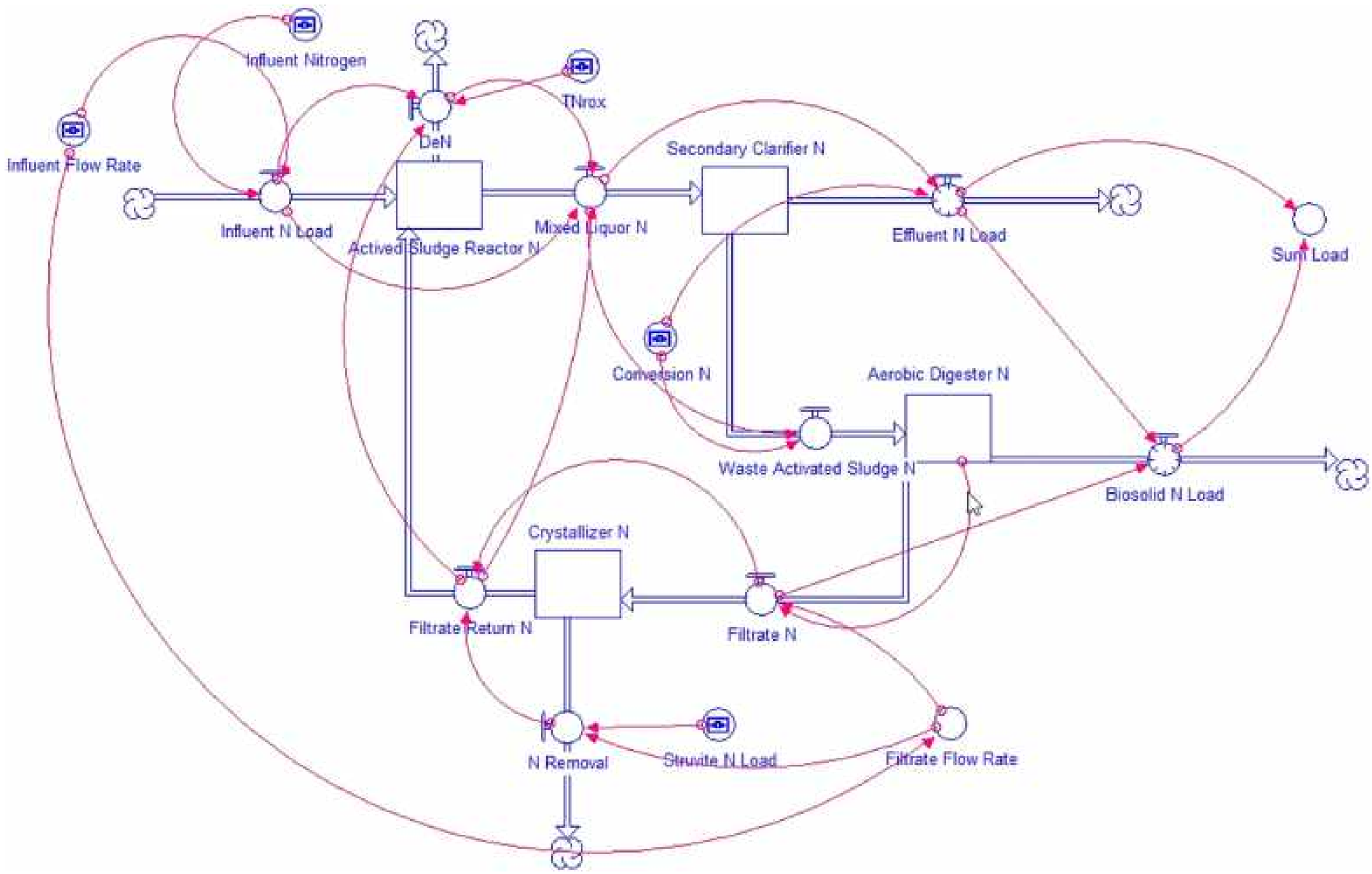

Fig. 2. Nitrogen mass balance model. Stocks (rectangle) and flows (pipe with tap) are the model's basic building blocks. Converters (small circles) represent calculations that link the flows and stock values.

2.4. Magnesium augmentation

A Mg model was not included, since the authors previously reported that under normal operational conditions, Mg concentration did not interfere with P or N balances (Hallas et al., 2019). However, Mg augmentation was used to optimize struvite yield. Two additional models were created in order to track Cl^- or SO_4^{2-} ions as by-products of Mg augmentation. These originated from either $MgCl_2$ or $MgSO_4$, respectively. The potential Cl^- and SO_4^{2-} transfer to effluent and waste activated sludge was calculated by mass balance from the experimental WWTP location data.

2.5. Statistical analyses

A mixed model method was used (JMP Pro, version 14.1.0, SAS Institute, Cary, NC, USA) for assessing results from the STELLA model runs. The STELLA model runs were subjected to the standard least squares method to determine the root mean square error (RMSE), which was used to evaluate model performance (Bennett et al., 2013).

3. Results

3.1. Model calibration and validation

Prior to including the struvite recovery component, calibration of each model was achieved by adjusting the corresponding conversion ratio. There was good agreement between measured data and modeled predictions (Table 3). The P model showed significant correlation of the modeled results with measured data at the $P < 0.05$ level, where $Y_{Modeled\ P} = 1.06X_{Measured\ P} + 0.01$ ($R^2 = 0.99$, $P < 0.001$), and RMSE = 0.047, indicating an overall agreement between measured and predicted data. Similarly, the N model showed a significant correlation of the modeled results with measured data at the $P < 0.05$ level, with $Y_{Modeled\ N} = 1.14X_{Measured\ N} - 0.44$ ($R^2 = 0.96$, $P < 0.001$), and RMSE = 1.9. The RMSE value was within expected ranges of N, indicating an overall agreement between measured and predicted data. Likewise, the Mg augmentation models for tracking Cl^- and SO_4^{2-} ions showed significant correlations of the modeled results with measured data at the $P < 0.05$ level, with $Y_{Modeled\ Cl} = 0.92X_{Measured\ Cl} + 0.63$ ($R^2 = 0.99$, $P < 0.001$) and $Y_{Modeled\ SO4} = 0.93X_{Measured\ SO4} + 0.11$ ($R^2 = 0.99$, $P < 0.001$), and RMSE = 1.1 and 0.3, respectively.

3.2. Phosphorus response to struvite addition

The experimentally determined struvite production rates from Table 1 were added to the P model. The resulting P reductions were somewhat similar between effluent and biosolids but percent

Table 3
Nutrient load comparisons between measured data and modeled results.

Parameters ($kg\ d^{-1}$)	Location 1		Location 2		Location 3	
	Measured	Modeled	Measured	Modeled	Measured	Modeled
Effluent P	7.0	7.0	2.3	2.3	2.7	2.8
Biosolids P	10.6	10.6	4.7	4.7	1.1	1.0
Effluent N	24.5	23.5	9.8	9.7	5.2	5.1
Biosolids N	27.5	27.5	9.0	9.0	0.7	0.6
Effluent SO_4^{2-}	6.7	7.3	5.5	5.5	0.45	0.45
Biosolids SO_4^{2-}	10.0	10.9	8.3	8.2	0.7	0.7
Effluent Cl^-	113	122	29.7	29.7	26.7	26.7
Biosolids Cl^-	3.5	3.8	0.9	0.9	0.8	0.8

Table 4
Modeled effect on effluent and biosolids P loads by including a struvite recovery module.

Scenario	Effluent P (kg P d^{-1})			Biosolids P (kg P d^{-1})		
	Location 1	Location 2	Location 3	Location 1	Location 2	Location 3
– Struvite	7.0	2.3	2.7	10.6	4.7	1.1
+ Struvite	0.0	1.4	1.7	8.8	3.7	0.6
+ Struvite +Mg	0.0	0.9	0.0	8.2	3.6	0.4

reductions in the outputs were relatively greater in the effluent (ranging from 0.9 to 7.0 kg P d^{-1} or 37–100%) compared to biosolids P (ranging from 0.5 to 1.8 kg P d^{-1} or 17–46%) (Table 4).

Hallas et al. (2019) reported that increasing [Mg^{2+}] to 1.5 times the P concentration approximately doubled struvite yield, and this relationship was used to calculate the amount of Mg^{2+} augmentation required for each location. The increased [Mg^{2+}] was used to calculate a new struvite production rate and this rate was applied to the models. The P model with the new struvite production rate predicted the P effluent load would be reduced 22% further at Location 2, and it would be completely eliminated from the effluent at Location 3 (Table 4). Location 1 was unaffected, as the effluent P load was eliminated without need for Mg augmentation. Additionally, the P biosolids load showed further reductions of 6%, 2%, and 18% for Locations 1, 2, and 3, respectively, through Mg augmentation (Table 4).

3.3. Nitrogen response to struvite addition

As with P, the experimentally determined struvite production rates from Table 1 were added to the N model. Removing N via struvite formation resulted in little to no additional reduction in effluent N for locations 1 and 2 but, with Mg augmentation, effluent N decreased 25% at location 3 (Table 5). In comparison, biosolids N was virtually unaffected by the inclusion of struvite production in the model.

The modeled results showed that the biosolids N:P ratio increased approximately 19% with Location 1 data, when the struvite module was included, and it increased by 27% if Mg augmentation was also included (Table 6). Location 2 had similar results with increases of 26 and 32%, respectively. In comparison, Location 3 N:P ratio increased 67% with a struvite module and 1.5 times when Mg augmentation was also included (Table 6).

3.4. Magnesium augmentation source effects

Using the struvite production rate for Mg augmentation, the Cl^- model showed modest percent increases in effluent and biosolids Cl^- loads across the three locations (Table 7). In comparison, the SO_4^{2-} model demonstrated that all three locations had substantial increases in effluent and biosolids SO_4^{2-} loads (Table 8).

Table 5
Modeled effect on effluent and biosolids N loads by including a struvite recovery module.

Scenario	Effluent N (kg N d^{-1})			Biosolids N (kg N d^{-1})		
	Location 1	Location 2	Location 3	Location 1	Location 2	Location 3
– Struvite	24.5	9.8	5.2	27.6	9.0	0.7
+ Struvite	24.0	9.2	4.7	27.1	9.0	0.6
+ Struvite +Mg	23.9	9.1	3.9	27.0	9.0	0.6

Table 6
Modeled effect on biosolids N:P ratio by including a struvite recovery module.

Scenario	Location 1	Location 2	Location 3
	N:P	N:P	N:P
– Struvite	2.6	1.9	0.6
+ Struvite	3.1	2.4	1.0
+ Struvite +Mg	3.3	2.5	1.5

Table 7
Modeled Cl^- loads.

Parameter	Location 1	Location 2	Location 3
Augmented effluent Cl^- (kg d^{-1})	132.3	31.4	27.7
% effluent load increase	17%	6%	4%
Augmented biosolids Cl^- (kg d^{-1})	4.1	1.0	0.9
% biosolids load increase	17%	11%	13%

4. Discussion

When the struvite component was added to the P model, results predicted that effluent and biosolids P would decline at all locations, including a complete elimination of effluent P discharged from Location 1. Location 1 had greater concentrations of N and P that resulted in proportionately greater struvite precipitation and a concomitant elimination of effluent P. This is a valuable behavior in terms of helping to address, cost-effectively, the water quality challenge of mitigating excessive ortho-P discharge from municipal water treatment. In order to improve the sustainability of municipal wastewater treatment, effluent nutrient discharge is a major concern (Roeleveld et al., 1997; Hospido et al., 2004). For example, reducing effluent P loads will lessen the impact of P-related eutrophication, which can cause the proliferation of dead zones, a decrease in aquatic biodiversity, and harmful algae blooms (Jarvie et al., 2006; Hendriks and Langeveld, 2017; Qi et al., 2020).

Struvite yields detailed by Hallas et al. (2019) were reported to cost \$80 per m^3 of wastewater treated. This is akin to P effluent reductions using chemical precipitation, such as granular activated aluminum (U.S. EPA, 2015). However, the struvite by-product is relatively pure and can be a valuable fertilizer product, while other types of chemical precipitation using metal salts (Al, Fe, and Ca) typically add to the sludge/biosolids mass and cost of disposal (Bertanza et al., 2013).

There was minimal impact on total N budgets by incorporating a struvite module. This is not surprising since N removal through biological denitrification typically accounts for 80% of influent N (Tchobanoglous et al., 2014), which represents significantly greater mass than the modeled N removal as struvite (Romero-Güiza et al., 2015).

The addition of a struvite recovery component to the models increased biosolids N:P ratios over 65% at one location and over 20% at the other two, principally by reducing biosolids P content. Increasing biosolids N:P ratios may benefit those who land-apply biosolids as fertilizer. For example, Location 1 biosolids fertilizer analysis was 5.9–5.3-0 (N-P_2O_5-K_2O). Based on the model results, struvite production may shift this to 5.9–4.1-0. A 20 kg P_2O_5 per hectare fertilizer application limit using 5.9–5.3-0 equates to 377 kg ha^{-1}, versus 488 kg ha^{-1} of 5.9–4.1-0, or 111 kg ha^{-1} more biosolids can be land-applied. Bahiagrass (*Paspalum notatum* Fluggé) pastures and hay fields represent over a million acres in Florida and are often major recipients of biosolids as fertilizer. For every 50 ha of biosolids-fertilized bahiagrass, the producer can apply an additional 5.55 Mg of 5.9–4.1-0. Taken a step further,

Table 8
Modeled SO_4^{2-} loads.

Parameter	Location 1	Location 2	Location 3
Augmented effluent SO_4^{2-} (kg d^{-1})	28.7	7.4	1.5
% Effluent load increase	328%	35%	231%
Augmented biosolids SO_4^{2-} (kg d^{-1})	43	11.1	2.2
% Biosolids load increase	330%	34%	214%

a third of biosolids produced in Florida are delivered to landfills. The ability to increase biosolids land-application rates over 20%, just by increasing the N:P ratio, may help divert nutrients essential for plant growth from landfills, while increasing the availability of limited landfill space for other materials.

Struvite itself, can be sold as commercial fertilizer, which might offset some of the WWTP operating costs. This added benefit may be attractive to smaller WWTPs especially, since they are not typically profitable services. Unlike biosolids, struvite is a completely inorganic mineral fertilizer, with a typical analysis of 5-28-0-10 (N-P_2O_5-K_2O-Mg). Although it has a much lower N:P ratio than biosolids, other characteristics increase its fertilizer value. For example, it is inorganic (contains no known organic contaminants), it has greater water solubility than biosolids and yet is not quite as soluble as most water-soluble P fertilizers. Additionally, this product can be packaged and stored in a manner similar to other conventional mineral fertilizers, thereby avoiding biosolids hauling costs (Woods et al., 2000).

Magnesium augmentation, used to increase struvite yields, also reduced and, in some cases, eliminated effluent ortho-P. However, selecting $MgSO_4^{2-}$ over $MgCl_2$ may result in excess effluent and biosolids S. Magnesium augmentation as $MgCl_2$ increased system Cl up to 17% and did not appear to pose any risk, whereas the sulfate from $MgSO_4$ augmentation increased system S up to 328% in some cases. Increased wastewater S loads might lead to a greater potential for H_2S formation and subsequently increase odor and corrosivity. Struvite production was equally as effective using $MgCl_2$ and, therefore, may be preferred.

5. Conclusions

Taking a system dynamics modeling approach to address WWTP nutrients led to predictions that incorporating struvite crystallization and recovery can significantly reduce or eliminate effluent P, while also lowering biosolids P content by a relatively smaller proportion. Even so, incorporating struvite production at small rural WWTPs will likely have a minimal effect on effluent and biosolids N loads. The resulting increase in biosolids N:P ratio may provide for proportionately greater biosolids land-application rates, particularly in locations with P application restrictions, such as Central Florida and the Northern Everglades region. This systems modeling tool may be utilized by WWTP operators who are considering whether intentional struvite crystallization will benefit their operation through primarily lessening nutrient P discharges into the downstream environment. Developing countries with limited municipal wastewater treatment technologies available could benefit from utilizing dynamic modeling tools to help assess nutrient processing and recovery options for increasing their environmental protection.

CRediT authorship contribution statement

John F. Hallas: Conceptualization, Methodology, Software, Validation, Formal analysis, Investigation, Data curation, Writing - review & editing, Visualization. **Cheryl L. Mackowiak:** Conceptualization, Methodology, Formal analysis, Resources, Data curation, Writing - review & editing, Visualization. **Ann C. Wilkie:** Conceptualization, Methodology, Formal analysis, Resources, Data curation, Writing - review & editing, Visualization.

Declaration of competing interest

The authors declare that they have no known competing financial interests or personal relationships that could have appeared to influence the work reported in this paper.

Acknowledgements

This research was supported by the Talquin Electric Cooperative, Inc., Quincy, Florida, USA.

References

ASTM International, 1995. ASTM D516-90(1995)e1. Standard Test Method for Sulfate Ion in Water. ASTM International, West Conshohocken, PA https://doi.org/10.1520/D0516-90R95E01.

AWWA, American Public Health Association, Water Environment Federation, 2012. In: Rice, E.W., Baird, R.B., Eaton, A.D., Clesceri, L.S. (Eds.), Standard Methods for the Examination of Water and Wastewater, 22 edition American Water Works Assn, Washington, DC.

Barbarick, K., Ippolito, J., McDaniel, J., 2017. Meta-analyses of biosolids effect in dryland wheat agroecosystems. J. Environ. Qual. 46, 452–460. https://doi.org/10.2134/jeq2016.12.0470.

Bennett, N.D., Croke, B.F.W., Guariso, G., Guillaume, J.H.A., Hamilton, S.H., et al., 2013. Characterising performance of environmental models. Environ. Model. Softw. 40, 1–20. https://doi.org/10.1016/j.envsoft.2012.09.011.

Bertanza, G., Pedrazzani, R., Manili, L., Menoni, L., 2013. Bio-P release in the final clarifiers of a large WWTP with co-precipitation: key factors and troubleshooting. Chem. Eng. J. 230, 195–201. https://doi.org/10.1016/j.cej.2013.06.067.

de Sousa, D.N.R., Mozeto, A.A., Carneiro, R.L., Fadini, P.S., 2014. Electrical conductivity and emerging contaminant as markers of surface freshwater contamination by wastewater. Sci. Total Environ. 484, 19–26. https://doi.org/10.1016/j.scitotenv.2014.02.135.

Elliott, H.A., Brandt, R.C., O'Connor, G.A., 2005. Runoff phosphorus losses from surface-applied biosolids. J. Environ. Qual. 34, 1632–1639. https://doi.org/10.2134/jeq2004.0467.

Elser, J., Bennett, E., 2011. A broken biogeochemical cycle. Nature 478 (7367), 29–31. https://doi.org/10.1038/478029a.

Filippelli, G.M., 2008. The global phosphorus cycle: past, present, and future. Elements 4, 89–95. https://doi.org/10.2113/GSELEMENTS.4.2.89.

Grady, C.P.L., Daigger, G.T., Lim, H.C., 1999. Biological Wastewater Treatment 2nd ed. rev. and expanded. Marcel Dekker, New York.

Hallas, J., Mackowiak, C.L., Wilkie, A.C., 2015a. Florida Biosolids: Management and Land Application Rules. Publication #SL421. UF/IFAS Florida Cooperative Extension Service, Gainesville, Florida http://edis.ifas.ufl.edu/SS634.

Hallas, J., Wilkie, A.C., Mackowiak, C.L., 2015b. Florida Biosolids: Rules for Biosolids Classes. Publication #SL422. UF/IFAS Florida Cooperative Extension Service, Gainesville, Florida http://edis.ifas.ufl.edu/SS635.

Hallas, J.F., Mackowiak, C.L., Wilkie, A.C., Harris, W.G., 2019. Struvite phosphorus recovery from aerobically digested municipal wastewater. Sustainability 11, 376. https://doi.org/10.3390/su11020376.

Hendriks, A.T.W.M., Langeveld, J.G., 2017. Rethinking wastewater treatment plant effluent standards: nutrient reduction or nutrient control? Environ. Sci. Technol. 51, 4735–4737. https://doi.org/10.1021/acs.est.7b01186.

Henze, M., Harremoës, P., la Cour Jansen, J., Arvin, E., 2002. Wastewater Treatment: Biological and Chemical Processes. 3rd ed. Springer-Verlag, Berlin.

Hospido, A., Moreira, M.T., Fernández-Couto, M., Feijoo, G., 2004. Environmental performance of a municipal wastewater treatment plant. Int. J. LCA 9, 261. https://doi.org/10.1007/BF02978602.

Jarvie, H.P., Neal, C., Withers, P.J.A., 2006. Sewage-effluent phosphorus: a greater risk to river eutrophication than agricultural phosphorus? Sci. Total Environ. 360, 246–253. https://doi.org/10.1016/j.scitotenv.2005.08.038.

Khalid, S., Shahid, M., Natasha, Bibi, I., Sarwar, T., et al., 2018. A review of environmental contamination and health risk assessment of wastewater use for crop irrigation with a focus on low and high-income countries. Int. J. Environ. Res. Public Health 15, 895. https://doi.org/10.3390/ijerph15050895.

Lahav, O., Telzhensky, M., Zewuhn, A., Gendel, Y., Gerth, J., et al., 2013. Struvite recovery from municipal-wastewater sludge centrifuge supernatant using seawater NF concentrate as a cheap Mg(II) source. Sep. Purif. Technol. 108, 103–110. https://doi.org/10.1016/j.seppur.2013.02.002.

Loewenthal, R.E., Kornmüller, U.R.C., van Heerden, E.P., 1994. Modelling struvite precipitation in anaerobic treatment systems. Water Sci. Technol. 30 (12), 107–116. https://doi.org/10.2166/wst.1994.0592.

Martinez-Moyano, I.J., 2018. A primer for system dynamics modeling and simulation. 2018 Winter Simulation Conference (WSC), Gothenburg, Sweden, 2018, pp. 261–275 https://doi.org/10.1109/WSC.2018.8632550.

Nowak, O., 2006. Optimizing the use of sludge treatment facilities at municipal WWTPs. J. Environ. Sci. Health A 41 (9), 1807–1817. https://doi.org/10.1080/10934520600778986.

O'Connor, G.A., Sarkar, D., Brinton, S.R., Elliott, H.A., Martin, F.G., 2004. Phytoavailability of biosolids phosphorus. J. Environ. Qual. 33, 703–712. https://doi.org/10.2134/jeq2004.7030.

Ohlinger, K.N., Young, T.M., Schroeder, E.D., 1998. Predicting struvite formation in digestion. Water Res. 32 (12), 3607–3614. https://doi.org/10.1016/S0043-1354(98)00123-7.

Qi, M., Yang, Y., Zhang, X., Zhang, X., Wang, M., et al., 2020. Pollution reduction and operating cost analysis of municipal wastewater treatment in China and implication for future wastewater management. J. Clean. Prod. 253, 120003. https://doi.org/10.1016/j.jclepro.2020.120003.

Roeleveld, P.J., Klapwijk, A., Eggels, P.G., Rulkens, W.H., van Starkenburg, W., 1997. Sustainability of municipal wastewater treatment. Water Sci. Technol. 35 (10), 221–228. https://doi.org/10.2166/wst.1997.0386.

Romero-Güiza, M.S., Astals, S., Mata-Alvarez, J., Chimenos, J.M., 2015. Feasibility of coupling anaerobic digestion and struvite precipitation in the same reactor: evaluation of different magnesium sources. Chem. Eng. J. 270, 542–548. https://doi.org/10.1016/j.cej.2015.02.057.

Silveira, M.L., O'Connor, G.A., Lu, Y., Erickson, J.E., Brandani, C., Kohmann, M.M., 2019. Runoff and leachate phosphorus and nitrogen losses from grass-vegetated soil boxes amended with biosolids and fertilizer. J. Environ. Qual. 48, 1498–1506. https://doi.org/10.2134/jeq2019.03.0106.

Snoeyink, V.L., Jenkins, D., 1980. Water Chemistry. Wiley, New York.

Tchobanoglous, G., Stensel, H.D., Tsuchihashi, R., Burton, F.L., Abu-Orf, M., et al., 2014. In: Metcalf & Eddy (Ed.), Wastewater Engineering: Treatment and Resource Recovery, Fifth edition McGraw-Hill Education, New York, NY.

U.S. EPA, 2015. A Compilation of Cost Data Associated With the Impacts and Control of Nutrient Pollution. US Environmental Protection Agency, Washington, DC, USA Document No. EPA 820-F-15-096. https://www.epa.gov/sites/production/files/2015-04/documents/nutrient-economics-report-2015.pdf.

Venkatesan, A.K., Hamdan, A.-H.M., Chavez, V.M., Brown, J.D., Halden, R.U., 2016. Mass balance model for sustainable phosphorus recovery in a US wastewater treatment plant. J. Environ. Qual. 45, 84–89. https://doi.org/10.2134/jeq2014.11.0504.

Wang, L.K., Shammas, N.K., Hung, Y.-T., 2007. Biosolids Treatment Processes. Humana Press, Totowa, NJ.

Wiener, M.S., Salas, B.V., Quintero-Núñez, M., Zlatev, R., 2006. Effect of H_2S on corrosion in polluted waters: a review. Corros. Eng. Sci. Technol. 41 (3), 221–227. https://doi.org/10.1179/174327806X132204.

Woods, N.C., Daigger, G.T., Sock, S.M., 2000. Sewage sludge reductions offered by phosphate recycling. Chim. Oggi-Chem. Today 18 (5), 68–70.

Zhao, T.-L., Li, H., Huang, Y.-R., Yao, Q.-Z., Huang, Y., et al., 2019. Microbial mineralization of struvite: salinity effect and its implication for phosphorus removal and recovery. Chem. Eng. J. 358, 1324–1331. https://doi.org/10.1016/j.cej.2018.10.139.